The Evolution of Large-Amplitude Internal Gravity Wavepackets

Sutherland, Bruce R. and Brown, Geoffrey L.

University of Alberta
Environmental and Industrial Fluid Dynamics Laboratory
Edmonton, Alberta, CANADA T6G 2G1
bruce.sutherland@ualberta.ca

Abstract :

The interaction between internal gravity wavepackets and their associated wave-induced mean flow is shown to dominate their weakly nonlinear evolution at early times. Sufficiently large amplitude waves either grow in amplitude as the wavepacket narrows or decrease in amplitude as the wavepacket broadens due to nonlinearly enhanced dispersion depending on whether the frequency is respectively greater or less than the frequency of internal waves having the fastest vertical group velocity. This is true whether the waves are horizontally periodic or horizontally compact. In non-uniformly stratified fluid, the weakly nonlinear effect acts to enhance or retard transmission of the waves across a localized evanescent region depending upon the wave amplitude and relative frequency.

Key-words :

internal gravity waves; weak nonlinearity; tunnelling

1 Introduction

Surface waves induce a mean flow known commonly as the Stokes drift. The maximum speed of this flow increases as the square of the wave amplitude but its influence back upon the waves is negligible even when the waves are close to breaking amplitude.

Likewise, vertically propagating internal wavepackets in continuously stratified fluid induce a horizontal mean flow, $U(z,t)$, whose vertical structure changes in time as the wavepacket propagates vertically and disperses. Unlike surface waves, however, the influence of the wave-induced mean flow back upon internal waves is non-negligible even when the waves are well below overturning amplitudes. At very large amplitude, the wave-induced mean flow can be larger than the horizontal group velocity of the wavepacket and thus drives the initially stable wavepacket into an overturning state (Sutherland (2001)). At moderately large amplitude the waves may remain stable, but the evolution of the wavepacket differs qualitatively from the propagation and dispersion characteristics predicted by linear theory.

Recently a nonlinear Schrödinger equation including high-order dispersion terms was derived and, by comparison with fully nonlinear numerical simulations, was shown to capture well the vertical structure of horizontally periodic internal wavepackets (Sutherland (2006)).

This paper shows how the horizontally periodic results can be extended to examine the evolution of internal wavepackets that are horizontally as well as vertically localized. This is done using fully nonlinear numerical simulations that focus specifically upon the case of non-hydrostatic waves having vertical wavenumber $m = -0.4k$, in which k is the fixed horizontal wavenumber. Such waves are modulationally unstable so that the wave-induced mean flow Doppler-shifts the waves to lower peak vertical wavenumber and larger maximum amplitude. We further examine the evolution of such wavepackets upon an unstratified finite-depth slab of fluid, thus extending linear theory predictions (Sutherland and Yewchuk (2004); Brown and Sutherland (2007)).

2 Weakly Nonlinear Theory

Generally, a one-dimensional, quasi-monochromatic wavepacket can be written in terms of its Fourier transform (Whitham (1974)):

$$A_\xi(z,t)\exp[\imath(mz-\omega_0 t)] = \int \hat{\xi}(\tilde{m})\exp[\imath(\tilde{m}z-\omega t)]\,d\tilde{m}, \tag{1}$$

In which A_ξ is the amplitude envelope of waves having vertical wavenumber m and frequency $\omega_0 \equiv \omega(m)$.

The influence of a mean flow, U, acting in the x-direction is including by replacing ω in (1) with the Doppler-shifted frequency $\Omega = \omega - Uk$. The methods of Hamiltonian fluid dynamics predicts that the leading order contribution to this wave-induced mean flow is given by (Scinocca and Shepherd (1992); Sutherland (2001))

$$U(z,t) \equiv -\langle \xi\zeta \rangle = -\frac{1}{2}\Re\{A_\xi {A_\zeta}^\star\}, \tag{2}$$

in which ξ is the vertical displacement, $\zeta = \partial_z u - \partial_x w$ is the vorticity, A_ξ and A_ζ are the corresponding complex-valued amplitude envelopes, and the angle brackets denote averaging over one horizontal wavelength. Using linear theory to write the amplitude of the vorticity field in terms of A_ξ, the explicit formula for the leading order contribution to the wave-induced mean flow is

$$U(z,t) = \frac{1}{2}N|\vec{k}||A_\xi|^2, \tag{3}$$

in which N is the buoyancy frequency and $\vec{k} = (k,m)$ is the wavenumber vector.

Thus we arrive at the following nonlinear Schrödinger equation:

$$A_t = -\omega' A_z + \imath\frac{1}{2}\omega'' A_{zz} + \frac{1}{6}\omega''' A_{zzz} - \imath\frac{1}{2}Nk|\vec{k}||A|^2 A, \tag{4}$$

in which primes denote m derivatives of ω and, for notational convenience, we have defined $A \equiv A_\xi$. The result, (4), was derived rigourously using perturbation theory (Sutherland (2006)).

On the right-hand side of (4), the first term represents propagation at the vertical group velocity, the next two terms represent linear dispersion and the last term introduces nonlinear effects due to the influence of the wave-induced mean flow upon the waves. For small-amplitude waves the last term is negligible. Compared with the second term, the third term is negligible for sufficiently wide wavepackets except for those moving near the speed of the maximum vertical group velocity, in which case $\omega'' = 0$. Solving the equation reveals that the third term is non-negligible even for finite-amplitude waves with $\Theta \simeq 0$ ($\omega \lesssim N$); it acts in concert with nonlinear effects to decrease the vertical group velocity.

3 Numerical Methods

The numerical simulations of two-dimensional, Boussinesq internal wavepackets solve the following coupled, fully nonlinear equations for the evolution of the vorticity and density fields (Sutherland (2006)):

$$\frac{D\zeta}{Dt} = -g\frac{\partial\rho}{\partial x} + \nu\nabla^2\zeta \tag{5}$$

and

$$\frac{D\rho}{Dt} = -w\frac{d\bar{\rho}}{dz} + \kappa\nabla^2\rho. \tag{6}$$

Here the constants g, ν and κ represent gravitational acceleration, kinematic viscosity and diffusivity, respectively. The last two are set to be sufficiently small to have negligible effect upon the wavepacket dynamics, but not so small that the code is numerically unstable. For an incompressible fluid, $\zeta = -\nabla^2\psi$ and the vertical velocity can be written in terms of the streamfunction by $w = \psi_x$. In uniformly stratified fluid, the fluctuation density can be written in terms of the vertical displacement field through the background density profile: $\rho = -(d\bar{\rho}/dz)\xi$.

The simulations are initialized by a internal wavepacket with k and m prescribed so the waves move upward in time. Generally we focus upon the evolution of Gaussian wavepackets with the vertical displacement field given initially by

$$\xi(x,z,0) = A(x,z,0)\cos(kx+mz) \text{ with } A(x,z,0) = A_0 \exp\left[-\frac{x^2}{2{\sigma_x}^2}\right]\exp\left[-\frac{z^2}{2{\sigma_z}^2}\right]. \quad (7)$$

For horizontally periodic waves, the prescribed initial background mean flow is given by computing the wave-induced mean flow using (2). The local horizontal flow associated with horizontally localized waves is prescribed by computing $-\xi\zeta$ everywhere in space and superimposing this on the horizontal velocity field. As the waves propagate, the corresponding horizontally averaged flow is found to move upward with the waves leaving behind no residual stationary mean flow.

In all simulations $\sigma_z k = 10$. In horizontally localized wavepacket simulations $\sigma_x k = 40$, and $\sigma_x k$ is treated as infinitely large for horizontally periodic waves. We focus upon finite-amplitude effects by examining waves with $A_0 k = 0.3$ and $m/k = -0.4$.

4 Results

4.1 Horizontally periodic waves

Figure 1 shows the evolution of a large amplitude, horizontally periodic wavepacket. Snapshots of the wavepacket at nondimensional times $Nt = 0$ and $Nt = 150$ (about 24 buoyancy periods) are shown in Figures 1a and b, respectively. The latter plot clearly shows that the nonlinear dynamics act to advect the waves differentially so that lines of constant phase tilt closer to the vertical where their amplitude is largest.

The corresponding vertical timeseries formed from successive profiles of the computed wave-induced mean flow, $U(z,t)$, is shown in Figure 1c. This reveals that the wavepacket moves upward initially at the vertical group velocity but, rather than broadening as expected from linear dispersion theory, the wavepacket narrows and the peak wave-induced mean flow increases to nearly double its initial value, U_0. The corresponding amplitude envelope increases by approximately 40%. At time $Nt \simeq 80$ the vertical propagation of the wavepacket slows and the pattern becomes considerably more complicated. At later times, there is little vertical advance while the maximum amplitude remains large.

In comparison with Figure 1c, Figure 1d shows timeseries of the strictly weakly nonlinear wavepacket evolution, which is found by solving (4). The initial development is the same as that determined from the fully nonlinear simulations with significant qualitative differences appearing only after $Nt \simeq 100$. At these late times the fully nonlinear wavepacket begins to undergo parametric subharmonic instability, which is apparent through the small vertical-scale structures superimposed on the large-scale wavepacket in Figure 1b.

Comparison of the simulation with weakly nonlinear theory serves to demonstrate that the interactions of waves with the wave-induced mean flow is the primary mechanism governing the initial evolution of finite-amplitude horizontally-periodic, vertically localized wavepackets.

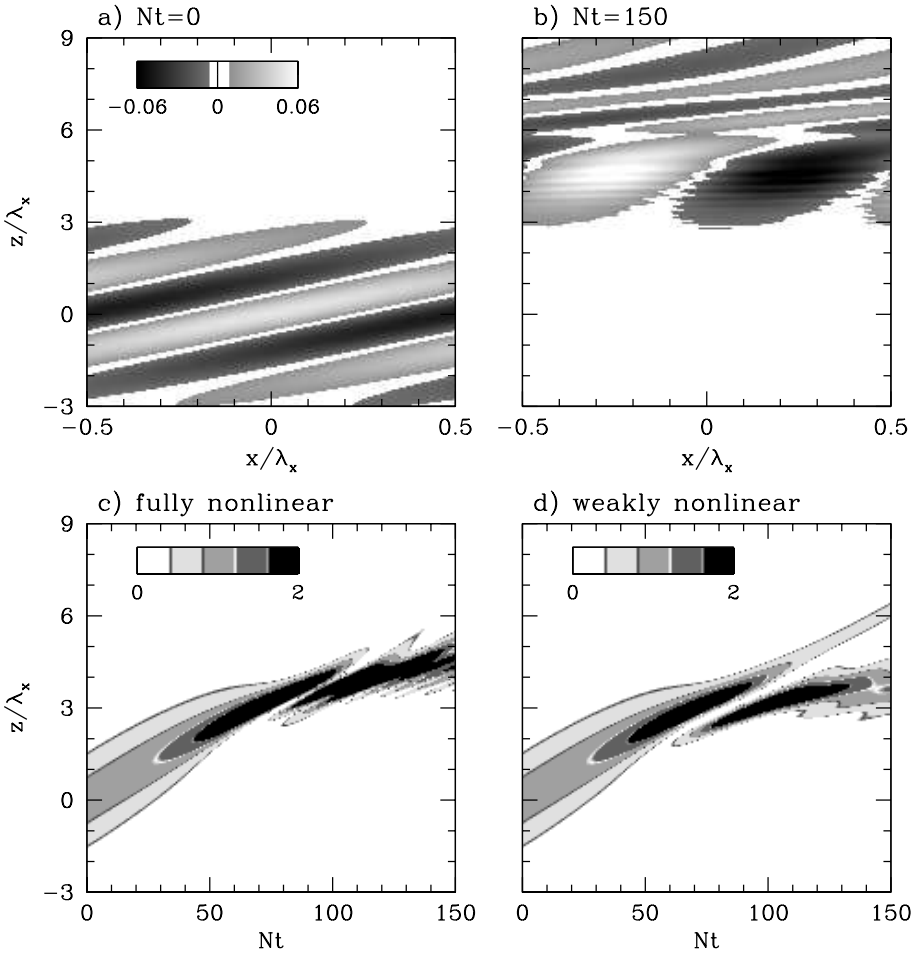

Figure 1: Results of a fully nonlinear numerical simulation of a wavepacket prescribed initially by (7) with $\sigma_z = 10k^{-1}$, $m = -0.4k$ and $A_0 = 0.3k^{-1}(\simeq 0.048\lambda_x)$ with the panels showing grayscale contours of the normalized vertical displacement field, ξ/λ_x, at times a) $t = 0$ and b) $t = 150N^{-1}$. Time series of the normalized wave-induced mean flow, $U(z,t)/U_0$, are computed c) from the fully nonlinear simulation and d) from weakly nonlinear theory. Here U_0 is the maximum wave-induced mean flow determined at the midpoint of the wavepacket at time $t = 0$.

We now go on to examine the influence of the mean flow acting over the horizontal extent of a horizontally localized wavepacket.

4.2 Horizontally localized waves

Figure 2 shows the results of a simulation of a wavepacket having the same characteristics as those of the internal wavepacket shown in Figure 1 but with finite horizontal extent prescribed by $\sigma_x = 40k^{-1}$. For ease of visualization, the snapshots are taken in a frame of reference moving with the horizontal group velocity as predicted by linear theory.

As with the horizontally periodic case, the wavepacket grows in amplitude and narrows as it propagates upward. However, because the wavepacket disperses horizontally, it takes longer for the growth in amplitude to occur. Over the time of the simulation, there is no substantial vertical deceleration of the wavepacket.

This simulation demonstrates that the wave-induced mean flow acting over the extent of the wavepacket has an influence upon the finite-amplitude evolution which is qualitatively similar

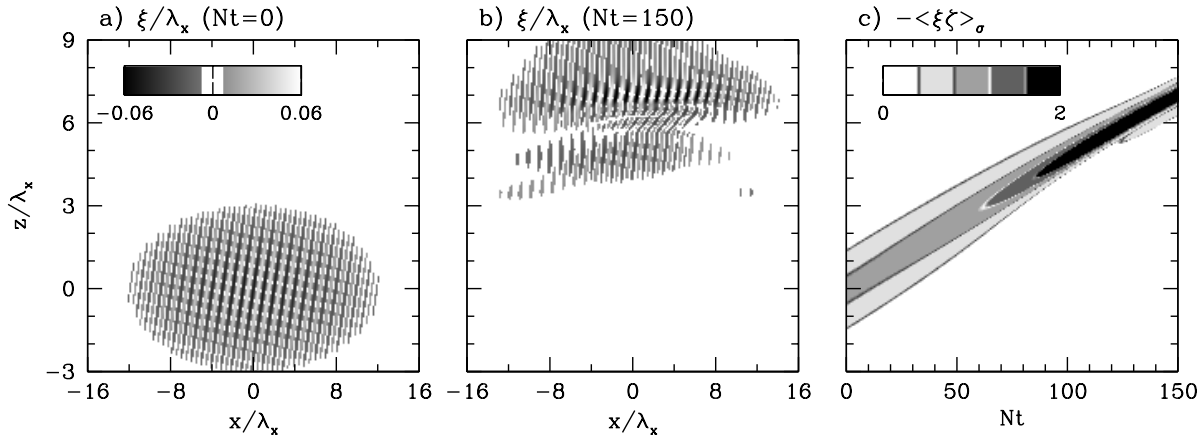

Figure 2: Simulation of a horizontally localized wavepacket run with same parameters as the simulation shown in Fig. 1 except with $\sigma_x = 40k^{-1}$. The plots show snapshots of the normalized vertical displacement field at times a) $Nt = 0$, b) $Nt = 150$ and c) the vertical timeseries of $-\langle\xi\zeta\rangle_\sigma / U_0$.

to that for horizontally periodic wavepackets.

In this case, however, the wave-induced mean flow is understood to refer to the flow acting over the extent of the wavepacket. Thus, similar to (2), we define $U = -\langle\xi\zeta\rangle_\sigma$ in which the subscript σ denotes averaging over the wavepacket width, $2\sigma_x$, rather than the horizontal extent of the domain.

Finally, we consider how these dynamics affect the evolution of a wavepacket propagating in non-uniformly stratified fluid. In particular, we examine a wavepacket propagating in a stationary fluid with buoyancy frequency, N, everywhere except in a slab of depth $L = 1k^{-1}$ situated between $z = 19.5k^{-1}$ and $20.5k^{-1}$ ($3.10\lambda_x \lesssim z \lesssim 3.26\lambda_x$) where the fluid is unstratified. Although the waves are evanescent in this region, the vertical extent of the slab is small enough that the waves can partially transmit across it through a process called tunnelling. Linear theory predicts the transmission coefficient is (Sutherland and Yewchuk (2004))

$$T = \left[1 + \left(\frac{\sinh(kL)}{\sin 2\Theta}\right)^2\right]^{-1}, \tag{8}$$

in which $\Theta = \tan^{-1}(m/k)$ is the angle at which lines of constant phase of the initial wavepacket are oriented with respect to the vertical. At fixed kL, the maximum transmission occurs for waves with $\Theta = 45^o$ ($m = k$). Our intent is to examine how the wave-induced mean flow affects the transmission of finite-amplitude waves.

The simulation results are shown in Figure 3. As occurs for small-amplitude waves (not shown), at late times the wavepacket splits into an upward propagating transmitted part and a downward propagating reflected part. However the proportion of the wavepacket that transmits is moderately smaller ($T = 25.6\%$) compared to the transmission coefficient waves with $A_0 = 0.3k^{-1}$ for which $T = 28.4\%$. As the waves approach the reflection level the amplitude doubles and so the wave-induced mean flow quadruples. Initially this acts to retard the transmission of waves. But as the waves reflect and the amplitude decreases, the Doppler-shifted frequency decreases, Θ becomes closer to 45^o and the transmission of the waves is enhanced.

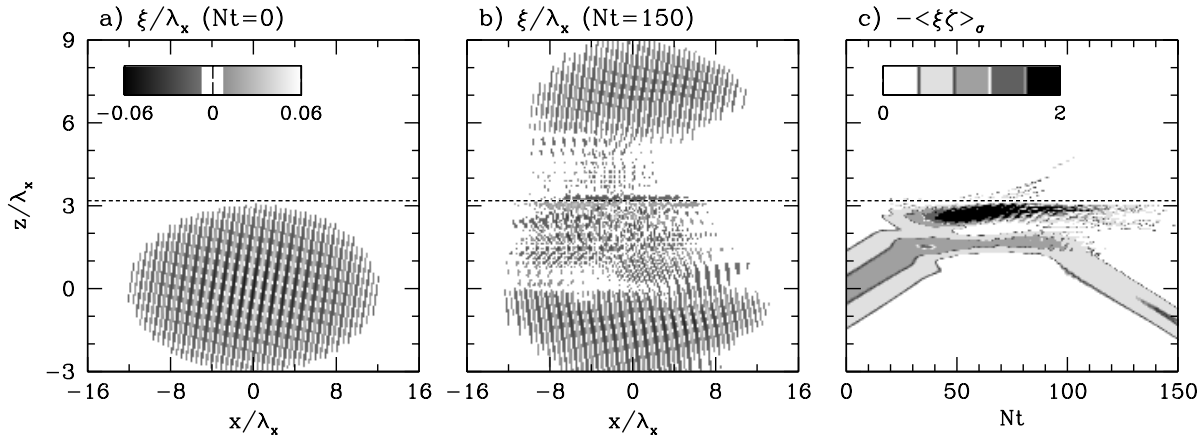

Figure 3: As in figure 2 but for a wavepacket incident upon an unstratified slab of fluid of depth $1k^{-1}$ ($\simeq 0.16\lambda_x$) centered about the position indicated by the dashed line.

5 Conclusions

We have focused upon a finite-amplitude wavepacket with specific characteristics in order to demonstrate that the primary weakly nonlinear mechanism governing its evolution is through the action of the wave-induced mean flow acting back upon the wavepacket. This is true whether the waves are horizontally periodic or horizontally compact. The feedback mechanism becomes more pronounced in non-uniformly stratified fluid, particularly where the waves approach a reflection level. This is because the magnitude of the wave-induced mean flow increases as the square of the wavepacket amplitude. The superposition of incident and reflected waves effectively double the wave amplitude and quadruple the influence of the wave-induced mean flow.

Acknowledgments The research was supported by the Canadian Foundation for Climate and Atmospheric Sciences (CFCAS).

References

Brown, G. L. and B. R. Sutherland 2007 Internal wave tunnelling through non-uniformly stratified shear flow. *Atmos. Ocean* in press

Scinocca, J. F. and T. G. Shepherd, 1992 Nonlinear wave-activity conservation laws and Hamiltonian structure for the two-dimensional anelastic equations. *J. Atmos. Sci.* **49** 5–27

Sutherland, B. R. 2001 Finite-amplitude internal wavepacket dispersion and breaking. *J. Fluid Mech.* **429** 343–380

Sutherland, B. R. 2006 Weakly nonlinear internal wavepackets. *J. Fluid Mech.* **569** 249–258

Sutherland, B. R. and K. Yewchuk 2004 Internal wave tunnelling. *J. Fluid Mech.* **511** 125–134

Whitham, G. B. 1974 *Linear and Nonlinear Waves*. pp. 636, John Wiley and Sons, Inc., New York.